International Conference on Space Optics—ICSO 2022

Dubrovnik, Croatia

3–7 October 2022

Edited by Kyriaki Minoglou, Nikos Karafolas, and Bruno Cugny,

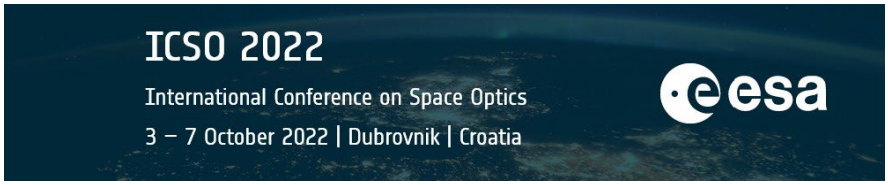

Designing transmit optical amplifiers for the current roll out of optical communication constellations

International Conference on Space Optics — ICSO 2022, edited by Kyriaki Minoglou, Nikos Karafolas, Bruno Cugny, Proc. of SPIE Vol. 12777, 127773H · © 2023 ESA and CNES · 0277-786X · doi: 10.1117/12.2690524

Designing transmit optical amplifiers for the current roll out of optical communication constellations

J. Edmunds, N. K. Thipparapu, M. Kechagias, K. Hall, A. Donnot, P. Kean, E. Kehayas, M. Welch.
G&H (Torquay), Broomhill Way, Torquay, Devon, TQ2 7QL, UK.

ABSTRACT

There are a number of parametric challenges in designing transmit optical amplifiers for the current deployment of optical communication constellations. Constellations are often aligned to channel wavelengths defined by the Space Development Agency (SDA) Tranche 1 Optical Communications Terminal Standard, which requires duplex operation at 1536.61 and 1553.33nm. We present an experimental characterisation supported by numerical modelling, of duplex operation up to 10W at both channel wavelengths and discuss performance limits. The characterisation includes power, out-of-channel amplified spontaneous emission (ASE) content and in-channel ASE content / noise figure determined from time-domain extinction measurements. For an output power of 10W, stimulated Brillouin scattering (SBS) can readily limit the delivery of optical power over relatively short fiber lengths. We also present the growth of a Stokes wave as a function of output power, delivery fiber length and fiber type experimentally. These results showing good agreement with theory, and set design limits on peak power transmission. These peak power considerations being of particular interest for pulse position modulation (PPM) encoding which are required in both the SDA and Consultative Committee for Space Data Systems (CCSDS) 142.0-B-1 standards. The CCSDS and SDA standards both require a sinusoid amplitude modulated tracking tone. We present the limits of the design space of achievable modulation depth, as function of amplifier design, modulation condition and operating wavelength & power. A good agreement between experimental and numerical results is found.

Keywords: Free Space Optical Communications, High power fiber amplifier, Er-doped fiber amplifier, Laser Communications, Space Photonics, Cubesats, Laser Transmitters, Constellations.

1. INTRODUCTION

There is an increasing activity within the space photonics industry as many satellite integrators express interest in incorporating optical links within their satellites due to the benefits that they can offer over traditional RF/microwave technology. The benefits of an optical link are well known and include higher data rates, lower system mass and higher security with an optical link being harder to intercept. Early developments of optical transmitters and amplifiers for space communication typically targeted <300mW output power and few Gbps operation [1-3] but higher data throughput, and higher optical powers are always sought. G&H have produced Watt level flight proven amplifiers, such as the high-power amplifier on LUCAS (Laser Utilising Communication System) [4, 5], and are amongst a number of companies are now rolling out commercial amplifier designs for the space market.

In this paper, we discuss some of optical design challenges of producing optical amplifiers for the current generation of constellations, focusing on key parametric performance challenges of the optical design. As discussed in the abstract, the challenges being discussed here, are the suppression of amplified spontaneous emission (ASE) whilst achieving high power amplification at 1536.61nm, the suppression of stimulated Brillouin scattering (SBS), the degradation of the required kHz sinusoid amplitude modulated tracking tone during amplification.

2. OPTICAL DESIGN

High throughput transmitters that would provide the data signal to the amplifier typically provide sub mW optical powers which can be as low as -10dBm. To robustly amplify this signal to 40dBm (10W) a three-stage amplifier should be employed. The experimental schematic shown in figure 1. initially comprises a high gain, low noise figure (NF) erbium (Er) amplification stage. The signal from which is spectrally filtered to remove ASE, before a low gain Er-doped amplifier stage which is operated in the strongly saturated regime to ensure a stable input signal into the final cladding pumped erbium/ytterbium (Er/Yb) stage.

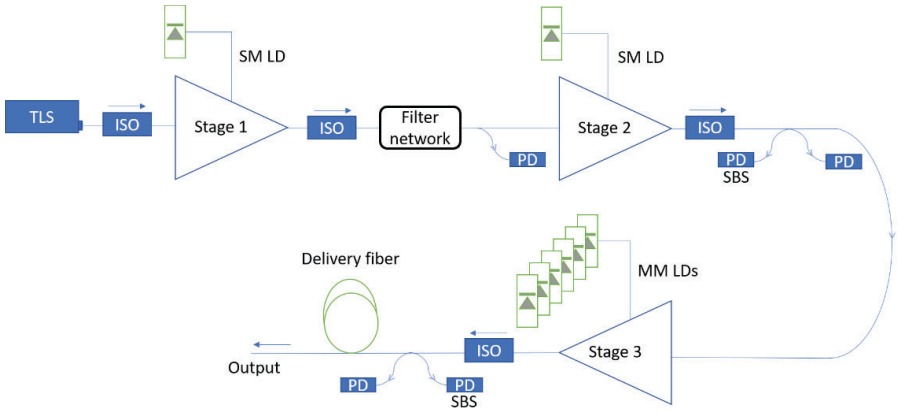

Figure 1. Schematic of 3-stage 10W single mode 1550nm amplifier.

A CW tunable laser source (TLS) is used as an input signal to the stage 1 of the master oscillator power amplifier (MOPA). Isolators (ISO) and taps were used to avoid back reflections and to monitor the power levels after each stage of the MOPA using photodiodes, respectively. Signal wavelengths of 1536.61nm and 1553.33nm defined by Space Development Agency (SDA) with signal powers from -10dBm to +5dBm being used for characterisation. Single mode laser diode (SM LD) operating at 976nm with a pump power of 350mW was used in a co-pumped configuration for stage 1. A single mode Er-doped fiber with an optimised length of 3m was used as a gain medium in stage 1, low noise amplifier. An output power of 19.6dBm and a gain of 29.6dB was obtained after stage 1 for a -10dBm of signal power at 1536.61nm.

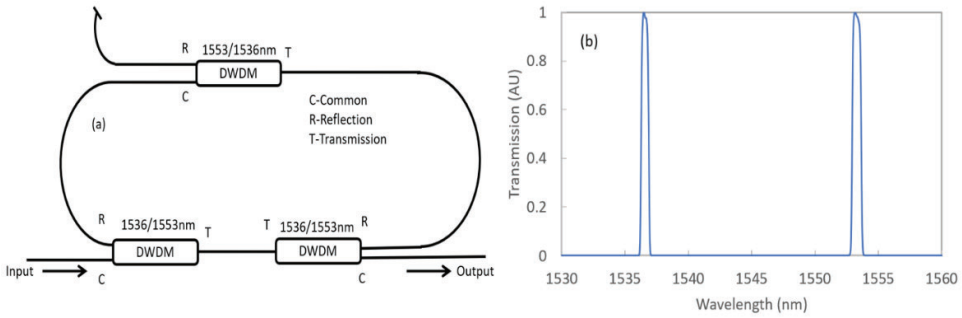

Figure 2. a) DWDM filter network, b) Transmission spectra of DWDM filter network.

The high gain of stage 1 induces high levels of ASE that would be amplified in subsequent stages reducing the output signal power. We have used a filter network as in figure 2. (a) to suppress out of band ASE after stage 1. The filter network was designed using two 1536/1553nm and one 1553/1536nm dense wavelength-division multiplexers (DWDMs). The transmission spectra of the filter measured with a 0.1nm resolution bandwidth optical spectrum analyser (OSA) is shown in figure 2. (b). The filter has transmission at central wavelengths around 1536.61nm and 1553.33nm with a bandwidth of 76.2 GHz and 74.5 GHz respectively. The insertion loss of the filter is about 0.9dB at both transmission wavelengths. An optimised 3m long single mode Er-doped fiber was used in stage 2 to boost the output of stage 1. Pump wavelength of 976 nm with a pump power of 350mW was used in a counter-pump configuration for stage 2. A maximum output power of 22dBm with a gain of 32dB was obtained at both 1536.61nm and 1553.33nm.

The power amplifier stage of the MOPA was pumped with six multi-mode pumps operating at 940nm. In stage 3 we have used a double clad Er/Yb-doped fiber. The length of the active fiber was optimised to obtain maximum output power as shown in figure 3. (a). An output power of 39.6dBm (9.2W) at 1536.61nm and 39.8dBm (9.6W) at 1553.33nm was obtained for a pump power of 30.8W. A maximum slope efficiency of 32% was achieved as shown in figure 3. (b). When the component losses in the output chain of stage 3 are taken into consideration, a raw efficiency from the amplifier of 41% is calculated which matches the highest reported values of commercial fibers. When run from a single 12V supply from G&H's micro controller and power conditioning interface (not shown) an E-O efficiency of 14% is achieved.

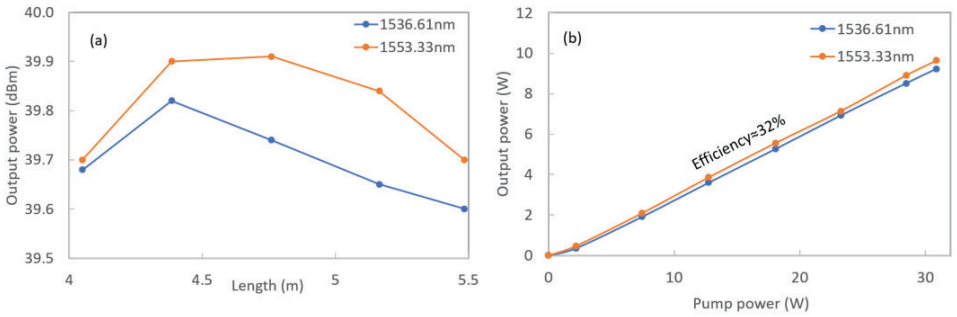

Figure 3. a) Output power with length of the active fiber and (b) Slope efficiency of stage 3.

3. NOISE FIGURE AND ASE CONTENT

The narrow bandwidth of the filter network within the amplifier makes it difficult to spectrally differentiate between the signal and the overlapping pedestal of ASE, with the resolution of a standard grating based OSA. Therefore, to measure the NF of the amplifier we have employed a time-domain extinction technique [6], this employed two acousto-optic modulators (AOMs), one to modulate the input signal and one to gate the sampled output signal, as shown in figure 4. Modulation of the input signal is performed at >1MHz frequencies, such that the gain of the amplifier (and therefore emitted ASE) is independent of the instantaneous input. Controlling the relative phase of AOMs allows the output spectra to be sampled with and without signal present, such that an output of just ASE or ASE plus amplified signal can be sampled.

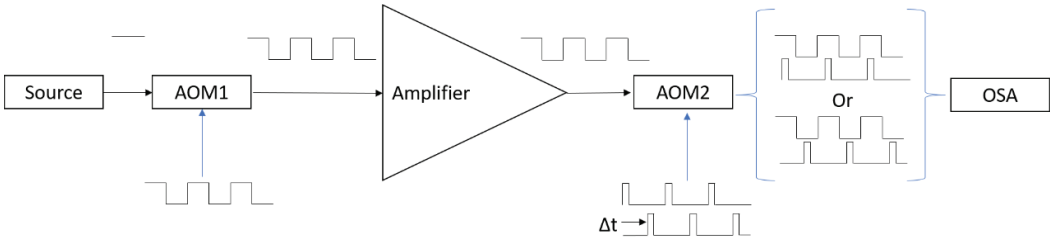

Figure 4. Schematic of the extinction technique to measure the noise figure of the amplifier.

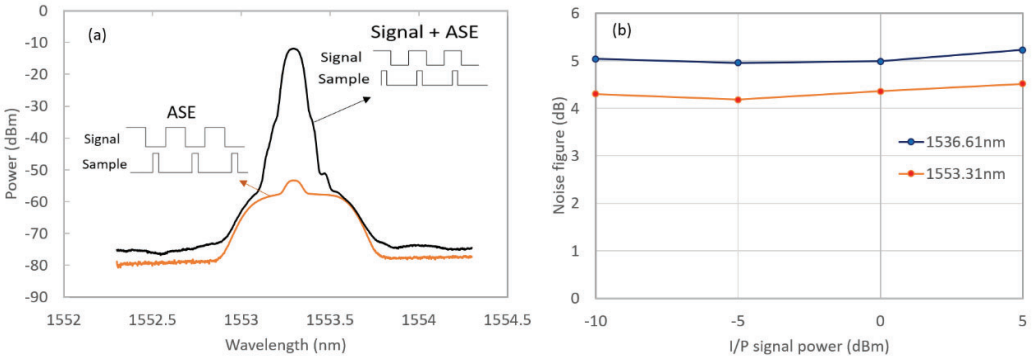

Figure 5. (a) Measured output spectra using time domain extinction technique, (b) Noise figure of MOPA using time-domain extinction technique for an output power of 39.1dBm.

Figure 5. (a) presents the measured output spectra using extinction technique. The ASE spectra shows the presence of signal power despite the high extinction ratio of the output AOM, which is nearly 50dB, though does not impede the measurement. A higher NF at 1536.61nm was measured compared to 1553.33nm, due to the higher signal reabsorption at this wavelength. Specifically, a minimum NF of 4.9dB was measured at 1536.61nm compared to 4.1dB at 1553.33nm for -5dBm of input signal power as shown in figure 5. (b).

We also measured the ASE spectrum over the c-band, to determine the ratio of integrated ASE power to signal. Operation at 1553.33nm is near the gain peak of the amplifier, and therefore leads to lower ASE levels than for 1536.61nm operation. Figure 6. (a) shows output spectrum for 1536.61nm operation, ASE levels are suppressed by the filter network apart from the pass band frequencies of 1536.61nm and 1553.33nm. The fractional power of ASE for all cases was less than 1%, as shown in figure 6. (b).

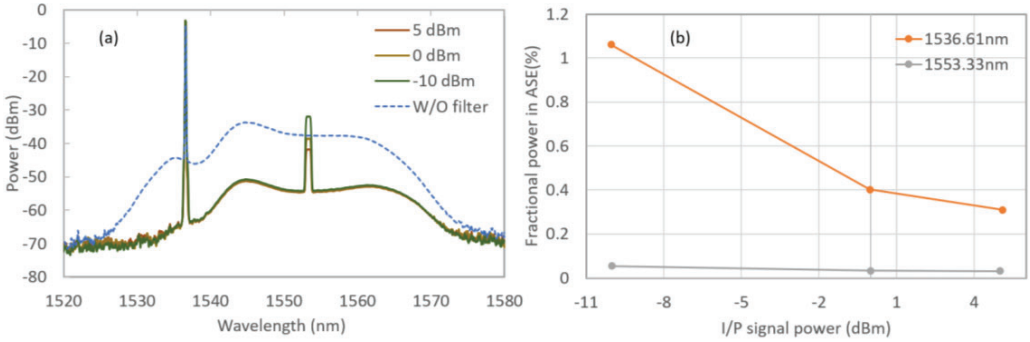

Figure 6. (a) ASE spectrum with 1536.61nm signal on (-10, 0, +5dBm) with and without filter, (b) Fractional power of ASE at 1536.61nm and 1553.33nm of the MOPA for an output power of 39.1dBm.

4. SBS EVALUATION

A key limitation of high-power fiber amplifiers is the onset of stimulated Brillouin scattering (SBS) especially when a narrow linewidth signal is amplified. In SBS, the propagating signal interacts with the medium and generates an optical wave downshifted in frequency (Stokes) and acoustic phonons. The generated acoustic phonons affect the medium's density and lead to a periodic modulation of refractive index, which strengthens the scattering of light into the Stokes wave. Various SBS mitigation techniques have been proposed in high power fiber amplifiers, out of which using a large mode area (LMA) fiber is the most common and simple technique [7-9]. LMA fibers increase the SBS threshold by lowering the intensity in the core. Here, we evaluate different delivery fibers with increasing core areas and therefore increasing SBS threshold: SMF28 (A_{eff} = 85µm^2), SCUBA150 (A_{eff} = 150µm^2) and 16µm (A_{eff} ≈ 220µm^2). To allow SBS to be characterised in all fibers, a 25m length was utilized, with them being individually connected to the output of the amplifier. The growth of the backwards propagating power being measured at a tap coupler, results being shown in figure 7 (a). In this figure, the power of the Stokes wave is initially below that of Rayleigh scattering and scattering from components, it becoming visible when the detected power exceeds approximately -60dBm.

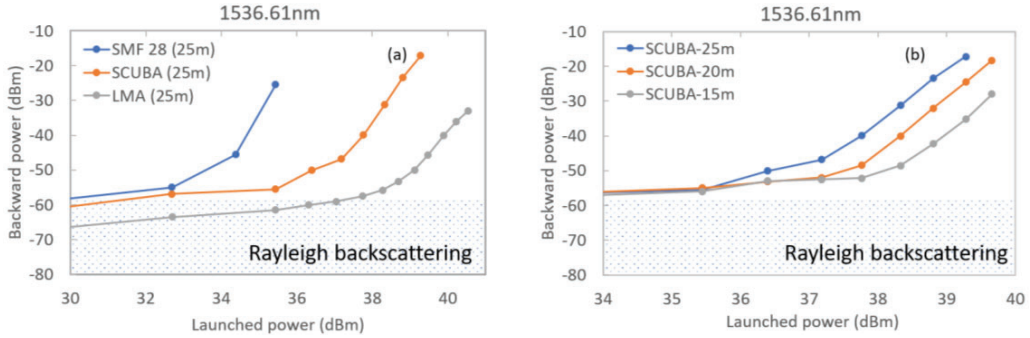

Figure 7. (a). SBS threshold for different types of delivery fibers, (b) SBS threshold of SCUBA150 fiber with length.

The measured SBS threshold for SMF28, SCUBA150 and 16µm LMA fibers are 34.4dBm, 37.1dBm and 39.1dBm respectively.

The theoretical SBS threshold is defined as [10, 11].

$$P_{Thres} = \frac{(21 * A_{eff})}{(L_{eff} * g_B * K)}$$

Where A_{eff} is the effective area of the fiber core, $L_{eff} = \frac{(1-e^{-\alpha L})}{L}$ is effective length of the fiber (accounting for loss), g_B=5E^{-11}m/W is peak value of Brillouin gain, K=0.5 is the polarisation factor. From this equation, theoretical SBS thresholds powers of 34dBm, 37dBm and 39dBm can be calculated for 25m lengths of SMF28, SCUBA150 and LMA fibers with close match to the measured values. The effect on reducing fiber length can also be observed in figure 7. (b) for the SCUBA fiber, with the threshold power reducing linearly with increases in fiber length as predicted by the above equation.

These tests were conducted with a CW, spectrally narrow input. Under pulsed operation, the peak power of the pulse should be used to calculate the SBS threshold. To this end if PPM data encoding is employed, as required by the SDS standard, then the SBS threshold can readily be reached for meter length scales, and large mode area fibers must be employed [12].

5. SINUSOID AMPLITUDE MODULATION

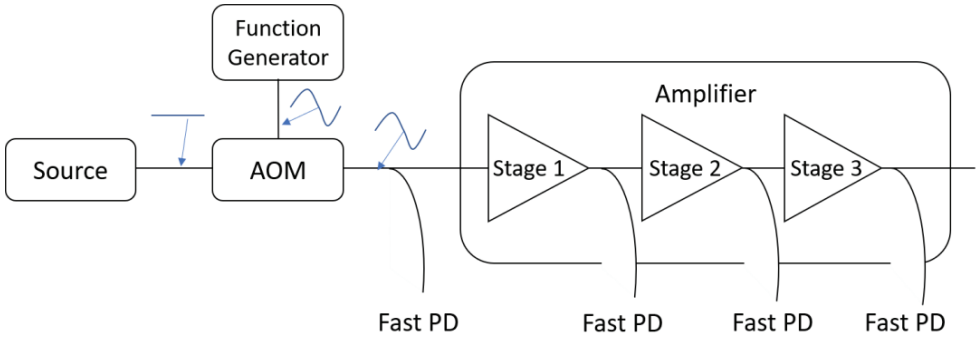

Figure 8. Schematic to study the impact of amplifier with sinusoidal input signal modulation.

CCSDS and SDA standards both require a sinusoid amplitude modulated tracking tone, the modulation frequency of this tone must be significantly lower than that of the data signal: in the tens to hundreds of kHz range. If this slow modulation is created by modulating the signal input of the amplifier, then modulation depth is not preserved during amplification, as amplifier gain varies across the tone. We present the limits of the design space of achievable modulation depth, as function of amplifier design, modulation condition and operating wavelength & power. The experimental schematic to study the frequency response of the amplifier for a modulated input signal is shown in figure 8. Here, we sinusoidally modulated the input signal using a function generator and an AOM. Different modulation frequencies (30kHz, 50kHz and 70kHz) with a modulation depth of 80% was used to evaluate the variation of modulation index (MI) of the output signal of the MOPA at 1536.61nm and 1553.33nm. The input and output temporal trace for different output powers at a 30kHz frequency are shown in figure 9. (a). One can observe that as the output power increases the modulation depth decreases, as the amplifier's gain is varying across the sinusoid.

Figure 9. (b) shows the MI variation, for different repetition rates, it shows for a given wavelength the modulation depth is related to the energy extracted per repetition. One can also observe that the degradation in MI is more significant in the case of 1536.61nm as compared to 1553.33nm. The situation is similar to that of pulsed optical amplifiers, where a saturation energy is typically quoted, this being the energy if instantaneously extracted would lead to a 1/e^2 drop in gain. Saturation energy can be theoretically calculated as:

$$\text{Saturation energy} = \frac{A\, h\nu}{(\sigma_{em} + \sigma_{abs})}$$

Where A is the mode area and σ_{em} & σ_{abs} are the wavelength dependent emission and absorption cross sections.

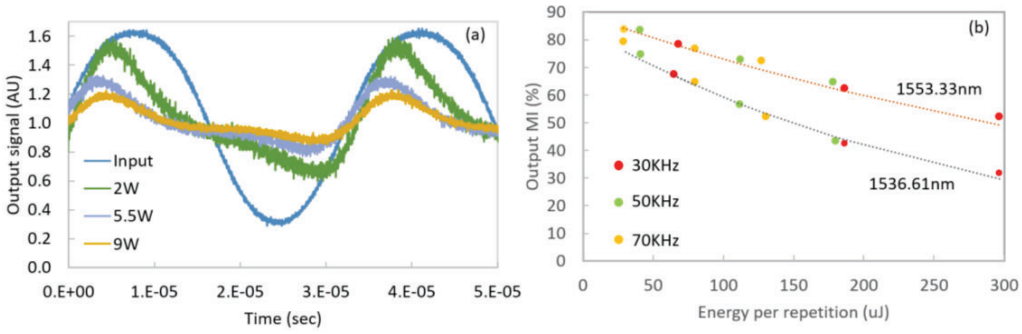

Figure 9. (a) Input and output signal at different output signal powers measured at the output of the amplifier, for a 30kHz sinusoid modulation, (b) Measured modulation index variation as a function of extracted energy per sinusoid period for 1536.61nm and 1553.33nm signal wavelengths.

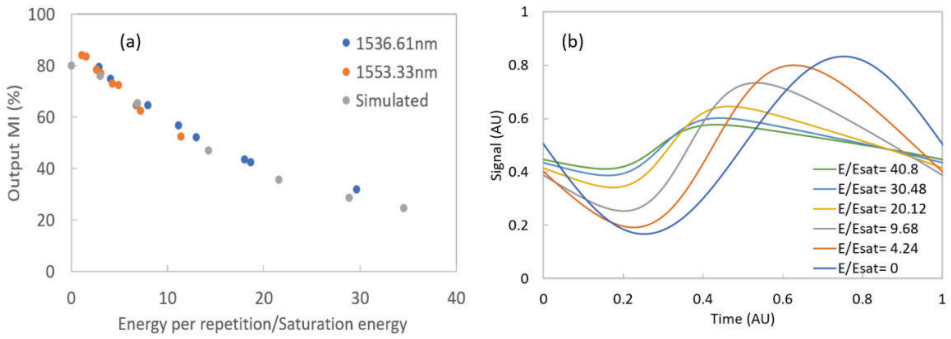

Figure 10. (a). Modulation index variation with pulse energy normalized to saturation energy, (b). Simulated temporal pulse shapes using RP Fiber Power.

Degradation of MI was measured to occur predominately in the final Er/Yb stage (data not shown), for this stage saturation, energies of 10µJ and 26µJ were calculated at 1536.61nm and 1553.33nm respectively. Figure 10. (a) shows the variation of MI with energy per repetition normalised to the saturation energy, which removed the wavelength dependence. Also shown are a series of simulations performed using RP Fiber Power considering signal sinusoidal modulation with different frequencies and compared with the experimental results as shown in figure 10. (a). The simulated results are well matched with the experimental results. Figure 10. (b) show example temporal pulse shapes from this modelling which match experimental traces in figure 9. (a).

From the data presented here, one can observe that if the required sinusoid modulated tracking signal is generated via slowly modulating the input signal then its degradation is linked to the saturation energy of the active fiber(s) employed. Shifting to larger mode area active fibers being key to increasing saturation energy, which is in keeping with requirement for larger mode area passive fibers required to mitigate SBS.

6. CONCLUSION

In this paper, we have studied some of the challenges that must be overcome in order to comply with the CCSDS and SDA standards at powers up to 10W. Spectral filtering was required to suppress ASE for operation at 1536.61nm, which meant that to measure the NF spectrally a time domain extinction method, must be employed. The SBS threshold of delivery fibers with different effective areas was measured and compared with the theoretical SBS threshold and good agreement found. The maintenance of a sinusoid amplitude modulated tracking tone during amplification at different modulation frequencies (30kHz, 50kHz and 70kHz) was assessed experimentally. We showed that saturation energy of the amplifier plays a critical role in degrading the MI of the output signal, with simulations being performed to support the experimental results and a good match is found between the experimental and simulation results.

ACKNOWLEDGEMENT

This work was supported by the Engineering and Physical Sciences Research Council [grant number EP/S022821/1].

REFERENCES

[1] E. Kehayas, J. Edmunds, J. Farzana, M. Kechagias and L. Stampoulidis, "Mid-power pm booster and optical fiber pre-amplifier for 1.55 um satellite laser communications," in International Conference on Space Optics - ICSO 2016, 2017.

[2] E. Kehayas, J. Edmunds, M. Welch, M. Tuci, C. Palmer, K. Simpson, R. Webb, M. Kechagias, L. Stampoulidis and C. Coopman, "Space qualification of multi-channel optical fiber amplifier for low Earth orbit satellite-to-ground direct downlinks," in Free-Space Laser Communication and Atmospheric Propagation XXX, 2018.

[3] L. Stampoulidis, J. Edmunds, M. Kechagias, G. Stevens, J. Farzana, M. Welch and E. Kehayas, "Radiation-resistant optical fiber amplifiers for satellite communications," in SPIE Proceedings, 2017.

[4] G&H, https://optics.org/news/11/12/39, 2020.

[5] Electrooptics.com, https://www.electrooptics.cosm/feature/looking-skyward-photonics-opportunities-space, 2022.

[6] D. M. Baney, P. Gallion and R. S. Tucker, "Theory and Measurement Techniques for the Noise Figure of Optical Amplifiers," Optical Fiber Technology, vol. 6, p. 122–154, April 2000.

[7] H. Lee and G. Agrawal, "Suppression of stimulated Brillouin scattering in optical fibers using fiber Bragg gratings," Optics Express, vol. 11, p. 3467, December 2003.

[8] Z. Lou, K. Han, X. Wang, H. Zhang and X. Xu, "Increasing the SBS threshold by applying a flexible temperature modulation technique with temperature measurement of the fiber core," Optics Express, vol. 28, p. 13323, April 2020.

[9] J. O. White, A. Vasilyev, J. P. Cahill, N. Satyan, O. Okusaga, G. Rakuljic, C. E. Mungan and A. Yariv, "Suppression of stimulated Brillouin scattering in optical fibers using a linearly chirped diode laser," Optics Express, vol. 20, p. 15872, June 2012.

[10] G. Agrawal, Applications of Nonlinear Fiber Optics, Academic Press, 2001.

[11] A. Kobyakov, M. Sauer and D. Chowdhury, "Stimulated Brillouin scattering in optical fibers," Advances in Optics and Photonics, vol. 2, p. 1, December 2009.

[12] A. Donnot, J. Edmunds, N. Hammond, M. Welch, P. Kean, E. Kehayas, R. Hagen, S. Yadav, H. Medenblik, L. Cheng, G. Bulgarini and M. Dresscher, “Development, assembly, and characterisation of a breadboard CCSDS compliant 4W average power high photon efficiency (HPE) pulsed laser source” in Free-Space Laser Communications XXXIV, 2022.